



## MINERALOGICAL CHARACTERIZATION OF SEDIMENTS, KALRAYAN HILLS SOUTH INDIA - A FTIR STUDY

Rajesh Paramasivam<sup>\*1</sup>, Senthil Shanmugam<sup>2</sup>, Ramasamy Venkidasamy<sup>3</sup>,  
Arivoli Shanmugam<sup>1</sup>

<sup>\*1</sup>PG and Research Department of Physics, Poompuhar college (AU), (Affiliated to Bharathidasan University),  
Melaiyur, Tamilnadu, India

<sup>2</sup>Department of Physics, Panimalar Engineering College, Poonamallee, Chennai, Tamilnadu, India

<sup>3</sup>Department of Physics, Annamalai University, Annamalainagar, Tamilnadu, India

<sup>4</sup>PG and Research Department of Chemistry, Poompuhar college (AU), (Affiliated to Bharathidasan University),  
Melaiyur, Tamilnadu, India

\*Corresponding author: [resh.tpm@gmail.com](mailto:resh.tpm@gmail.com)

### ABSTRACT

In environmental studies, the mineralogical composition of sediments is an important indicator. In combination with other indicators, they contribute to the understanding of changes in sediment sourcing as well as in weathering and depositional processes. Fourier transform infrared spectroscopy (FT-IR) spectra contain information on mineralogical composition because each mineral has a unique absorption pattern in the mid-IR range. In this study, total of sixty five sediment samples were collected from different locations of the Kalrayanhills, part of Eastern ghats, South India, lies between the north latitudes 11° 36' and 12° 01' N and the east longitudes 78° 29' and 78° 54' E. Twenty three minerals are identified using FT-IR analysis. Obtained minerals are confirmed by X-ray diffraction (XRD) analysis. The relative distribution of major minerals was determined by calculating extinction co-efficient.

**Keywords:** Mineralogy, FTIR, Extinction co-efficient, Sediments, Kalrayan hills.

### 1. INTRODUCTION

Hills are one of the valuable natural source of various ore minerals, incorporating a large group of metals necessary for an increasing number of industrial and technological applications [1]. Ramasamy et al., [2] reported that, minerals related industrial developments help to grow the national economy. The knowledge of mineral composition of rock and sediments is very important in quartz processing. Many of these resources are not uniformly distributed, in horizontal space and vertical depth. Their quantitative occurrences are also highly varied. New advances have already been achieved [3, 4], however additional work is required to suitably address the highly varied mineral assemblages, incorporating valuable by-products and the fingerprints or footprints that should be used in modern exploration surveys oriented to concealed ore minerals systems.

Fourier transform infrared (FT-IR) spectroscopic techniques are most commonly developed for qualitative studies, careful examination of intensities leads to a most useful tool for quantitative analysis as well [1]. One of the

most important and value added applications of the infrared spectroscopic study is the identification of the minerals in the rock and sediment samples. In the present study, an attempt has been made to characterize the minerals present in the sediment samples from Kalrayan Hills, South India.

### 2. MATERIAL AND METHODS

#### 2.1. Sampling and Preparation

The present study area is part of Kalrayan hills, it starts right from Vandagappadi (Lat: 11°49' 102; Long: 78°46' 418) to Kallippattu (Lat: 11°51' 824; Long: 78°47' 900). It spreads over an area of 1095 Sq. Km. It acts as catchment for Gomukhi, Kariakovil and Manimuktha rivers. This covers three districts namely Villupuram, Salem and Dharmapurai of Tamilnadu. Total of sixty five samples were collected from different locations of the study regions. The sample location were recorded in terms of degree-minute-decimals (Latitudinal and Longitudinal position) using Hand-held Global Positioning System (GPS) (Model: GARMIN GPS-12)

unit. Each location is separated by a distance of 5-6 km approximately and is numbered as S<sub>1</sub> to S<sub>65</sub> for sediment samples. Sampling locations in the study area is shown in

Fig. 1. The collected samples were air dried at room temperature in open air.

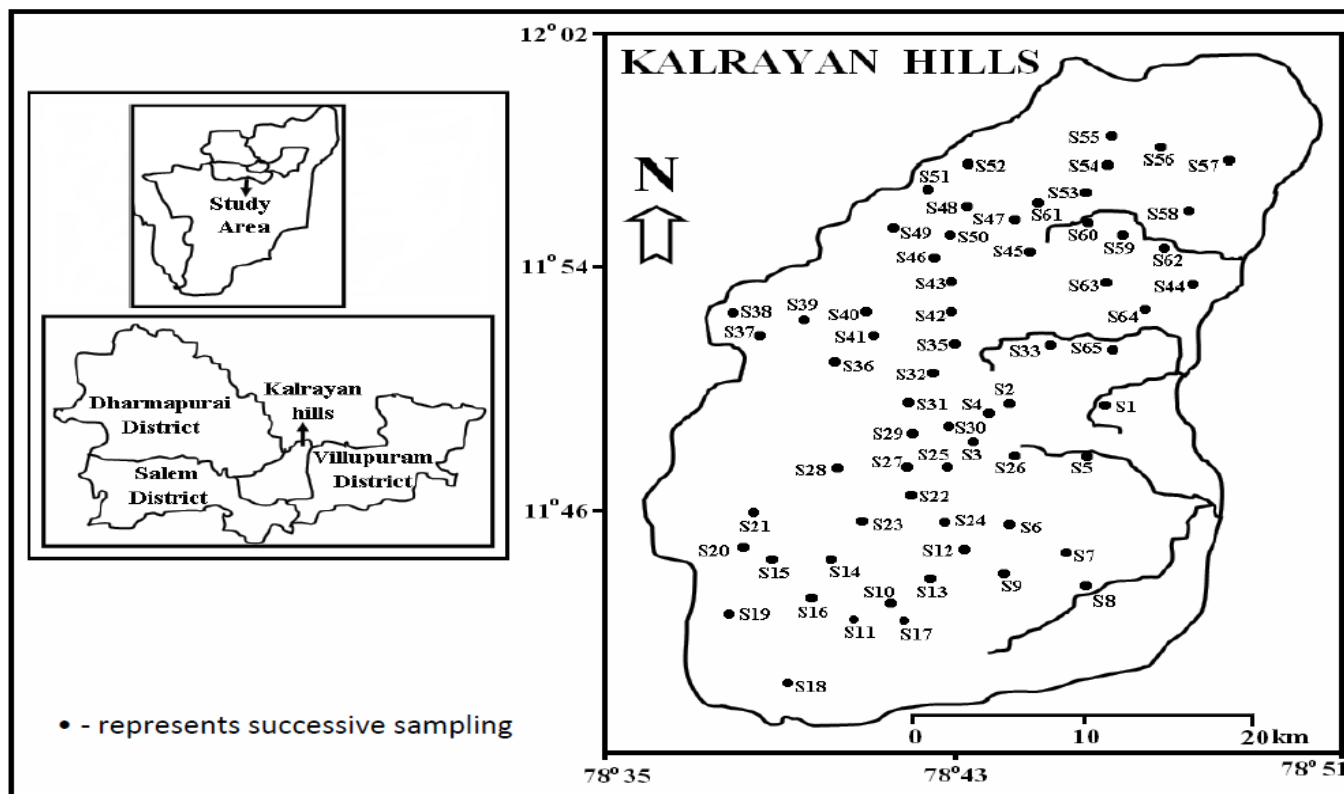


**Fig. 1: Location of Kalrayan hills with their experimental sites in Tamilnadu, South India**

All the collected samples were subjected to various pre-treatment in order to remove organic matter and certain other materials for improving the quality and for resolution of the spectra. The KBr pellet technique was used in the present investigation. All chemicals used were of spectroscopic grade.

Materials required for KBr pressed-pellet method are Potassium Bromide (KBr), acetone, die for making pellets, laboratory hydraulic press for creating pressure on the confined sample, small hand agate mortar and pestle and mechanical vacuum pump. Wet grinding was carried out by placing 30 to 50 mg of the sample in an agate mortar along with 20 to 25 drops of ethanol. The ground samples were dried in a hot air oven at 110°C to remove the moisture content. Using the KBr pellet technique, each grain sized sample was mixed with KBr at various ratios viz., 1:10, 1:20, 1:30, 1:40 and 1:50. The mixture was then pressed into a transparent disc in an evacuable dye at sufficiently high pressure. The samples in the ratio 1:30 (sample: KBr) was taken for further analysis, since it gives rise to maximum

transmittance and observable peaks [5]. This ratio was checked for 2 to 3 times for its accuracy.

For XRD study, selected sediments samples were taken for analysis. The samples ground by an agate mortar and sieved to 53 µm meshes were used.

## 2.2. FTIR

Using the Perkin Elmer RX1 FTIR spectrometer, the infrared spectra for all the samples were recorded in the region 4000-400 cm<sup>-1</sup> at room temperature. It scans the spectra 100 times in 1 minute. The resolution of the instruments is 0.001cm<sup>-1</sup> and the accuracy is ±4 cm<sup>-1</sup>. At each and every time, this instrument was calibrated for its accuracy with the spectrum of a standard polystyrene film.

## 2.3. XRD

The X-ray diffraction powder pattern of selected samples was recorded at room temperature using Seifert (JSO-DEBYEFLEX 2002). X-ray diffractometer having a curved graphite crystal diffracted monochromator,

with a source of CuK $\alpha$  radiation and NaI (Tl) scintillation detector.

**2.4. Relative Distribution Of Major Minerals**

The relative distribution can be quantified by calculating the extinction co-efficient using the formula [2].

$$K = DA/m$$

Where K is the extinction co-efficient, A is the area of the pellet and m is the mass of the pellet. D is the optical density.

**3. RESULTS AND DISCUSSION**

**3.1. Determination and characterization of minerals**

The FTIR spectra for all the sediment samples were recorded. A selected representative FT-IR spectrum of the sediment samples (S<sub>4</sub>) are shown in Fig. 2. The observed wave numbers are analyzed and the minerals are assigned using available literatures [2, 6-13]. The observed wave numbers from all the spectra are given in the Table 1 along with their corresponding mineral names.

Twenty three minerals are identified through FT-IR analysis. These minerals such as quartz, feldspar in different composition (microcline, orthoclase and albite), hematite, Kaolinite, palygroskite, magnetite, maghemite, biotite, gibbsite, montmorillonite, calcite, aragonite, illite, lepidocrocite, ferrihydrate, hornblende, nacrite, sepiolite, chrysotile, cerussite and organic carbon are identified in sediment samples. The various bands in the region 3000-3800 cm<sup>-1</sup> are all due to OH stretching and in the region 1600 - 1700 cm<sup>-1</sup> are due to OH bending modes of water or hydroxyls.

No additional features are observed in this region. The bands in the region 1420-1460 cm<sup>-1</sup> are due to the presence of carbonate minerals. The variations in the values of OH stretching and bending wave numbers from sample to sample are usually attributed to the varying strength of hydrogen bonding between OH and H<sub>2</sub>O molecules and some oxygen in the structure. The present results with few exceptions are in fairly good agreement with the absorption maxima in the recorded survey of silicate, non-silicate and carbonate minerals by [8-10, 14].

**Table 1: The observed absorption wave numbers and corresponding minerals from FTIR spectra**

Sl. No.	Name of the minerals	Site number	Observed wave numbers (cm <sup>-1</sup> )
1	Quartz	S <sub>1</sub> -S <sub>65</sub>	460-462
		S <sub>33</sub> -S <sub>34</sub> , S <sub>37</sub> , S <sub>47</sub> , S <sub>54</sub> , S <sub>56</sub> -S <sub>57</sub> and S <sub>60</sub>	510-514
		S <sub>1</sub> - S <sub>29</sub> , S <sub>31</sub> -S <sub>37</sub> , S <sub>40</sub> -S <sub>45</sub> and S <sub>62</sub>	693-695
		S <sub>1</sub> - S <sub>65</sub>	777-779
		S <sub>1</sub> - S <sub>8</sub> , S <sub>20</sub> , S <sub>23</sub> - S <sub>65</sub>	794-796
		S <sub>4</sub> - S <sub>23</sub> , S <sub>33</sub> -S <sub>37</sub> , S <sub>40</sub> , S <sub>42</sub> - S <sub>45</sub> , S <sub>49</sub> - S <sub>52</sub> , S <sub>56</sub> - S <sub>65</sub>	1080-1086
		S <sub>23</sub> , S <sub>34</sub> - S <sub>36</sub> , S <sub>43</sub> - S <sub>44</sub> , S <sub>48</sub> , S <sub>52</sub> , S <sub>56</sub> , S <sub>61</sub> - S <sub>65</sub>	1160-1164
		S <sub>1</sub> - S <sub>37</sub> , S <sub>40</sub> , S <sub>46</sub> , S <sub>48</sub> , S <sub>51</sub> - S <sub>65</sub>	1610-1614
		S <sub>1</sub> - S <sub>29</sub> , S <sub>31</sub> - S <sub>37</sub> , S <sub>40</sub> , S <sub>43</sub> - S <sub>48</sub> , S <sub>51</sub> - S <sub>65</sub>	1870-1875
2	Microcline Feldspar	S <sub>1</sub> - S <sub>65</sub>	585- 588
3	Orthoclase Feldspar	S <sub>1</sub> - S <sub>65</sub>	633-638
4	Hematite	S <sub>1</sub> - S <sub>65</sub>	535-539
		S <sub>19</sub> - S <sub>22</sub> , S <sub>33</sub> , S <sub>49</sub> - S <sub>50</sub> and S <sub>59</sub>	1012-1016
		S <sub>1</sub> - S <sub>22</sub> , S <sub>24</sub> - S <sub>32</sub> , S <sub>36</sub> - S <sub>42</sub> , S <sub>44</sub> - S <sub>48</sub> , S <sub>22</sub> - S <sub>55</sub> - S <sub>56</sub> , S <sub>58</sub> and S <sub>61</sub>	1034-1037
		S <sub>1</sub> - S <sub>65</sub>	3400-3405
		S <sub>19</sub> and S <sub>21</sub>	3367-3368
		S <sub>13</sub> - S <sub>16</sub> , S <sub>20</sub> - S <sub>30</sub> , S <sub>36</sub> , S <sub>39</sub> - S <sub>40</sub> , S <sub>43</sub> , S <sub>46</sub> - S <sub>48</sub> , S <sub>52</sub> - S <sub>53</sub> , S <sub>55</sub> and S <sub>61</sub>	3618-3620
5	Kaolinite	S <sub>13</sub> - S <sub>16</sub> , S <sub>20</sub> , S <sub>23</sub> , S <sub>26</sub> , S <sub>30</sub> , S <sub>36</sub> , S <sub>39</sub> , S <sub>40</sub> , S <sub>43</sub> , S <sub>46</sub> - S <sub>48</sub> , S <sub>52</sub> - S <sub>53</sub> , S <sub>55</sub> and S <sub>61</sub>	3652-3656
		S <sub>5</sub> , S <sub>26</sub> , S <sub>30</sub> , S <sub>35</sub> , S <sub>42</sub> , S <sub>47</sub> , S <sub>54</sub> , S <sub>56</sub> and S <sub>57</sub>	574
		S <sub>4</sub> , S <sub>9</sub> , S <sub>30</sub> , S <sub>35</sub> and S <sub>56</sub>	723-727

8	Biotite	S <sub>5</sub> , S <sub>9</sub> - S <sub>11</sub> , S <sub>19</sub> , S <sub>23</sub> , S <sub>24</sub> , S <sub>26</sub> , S <sub>28</sub> , S <sub>30</sub> , S <sub>35</sub> , S <sub>41</sub> , S <sub>42</sub> , S <sub>46</sub> , S <sub>47</sub> , S <sub>53</sub> - S <sub>57</sub> , S <sub>59</sub> and S <sub>60</sub>	720 -724
9	Palygorskite	S <sub>41</sub> , S <sub>43</sub> - S <sub>44</sub> S <sub>1</sub> - S <sub>53</sub> , S <sub>55</sub> - S <sub>59</sub> , S <sub>61</sub> -S <sub>65</sub>	514-517 1636-1639
10	Gibbsite	S <sub>1</sub> - S <sub>65</sub>	668-670
11	Montmorillonite	S <sub>5</sub> , S <sub>18</sub> , S <sub>21</sub> , S <sub>35</sub> , S <sub>49</sub> and S <sub>62</sub>	875 -878
12	Albite	S <sub>30</sub> and S <sub>53</sub>	1006-1010
13	Calcite	S <sub>7</sub> , S <sub>12</sub> -S <sub>14</sub> , S <sub>22</sub> , S <sub>24</sub> , S <sub>29</sub> , S <sub>34</sub> , S <sub>36</sub> , S <sub>43</sub> , S <sub>52</sub> -S <sub>53</sub> , S <sub>58</sub> and S <sub>62</sub>	1423-1428
14	Aragonite	S <sub>7</sub> , S <sub>12</sub> -S <sub>14</sub> , S <sub>22</sub> , S <sub>29</sub> , S <sub>36</sub> , S <sub>52</sub> -S <sub>53</sub> , S <sub>58</sub> and S <sub>62</sub>	1784-1789
15	Illite	S <sub>30</sub> and S <sub>39</sub>	749-754
16	Lepidocrocite	S <sub>5</sub> , S <sub>35</sub> , S <sub>56</sub> and S <sub>59</sub>	544-548
		S <sub>4</sub> , S <sub>26</sub> and S <sub>56</sub>	1018-1022
		S <sub>4</sub> , S <sub>26</sub> and S <sub>56</sub>	1151
17	Ferrihydrate	S <sub>56</sub>	970-973
18	Hornblende	S <sub>5</sub> and S <sub>56</sub>	662-664
19	Nacrite	S <sub>7</sub> , S <sub>29</sub> , S <sub>58</sub> and S <sub>62</sub>	914 - 917
20	Sepiolite	S <sub>12</sub> -S <sub>13</sub> and S <sub>62</sub>	423 - 453
21	Chrysotile	S <sub>40</sub>	450 - 453
22	Cerussite	S <sub>52</sub>	1394 - 1398
23	Organic carbon	S <sub>1</sub> -S <sub>65</sub>	2854 - 2857
		S <sub>1</sub> -S <sub>65</sub>	2924 - 2928

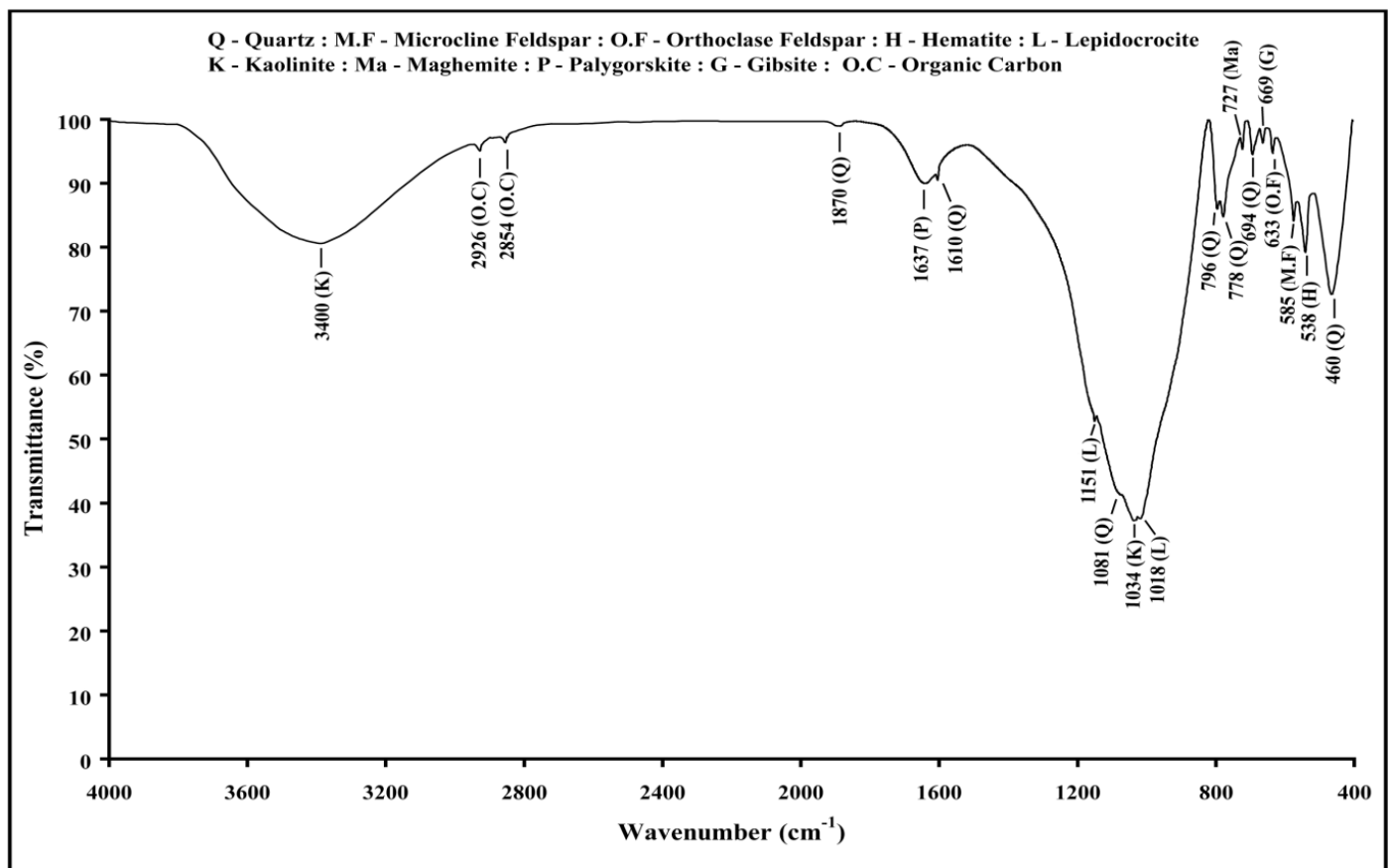


Fig. 2: FTIR spectrum of site number S<sub>4</sub>

### 3.2. Quartz

The silicate minerals are of primary concern because of their relative abundance and importance. Quartz is a non-clay mineral, which is common and invariably present in all the samples. The Si-O bonds are the strongest bonds in the silicate structure and can be readily recognized in the infrared spectra of such minerals by very strong bands in the region 900 to 1100  $\text{cm}^{-1}$  (stretching) as well as less intense bands in the 400 to 800  $\text{cm}^{-1}$  region (bending). The presence of quartz in the samples can be ascribed by the observation of the peaks in the ranges 460-462 and 510-514  $\text{cm}^{-1}$  due to Si-O asymmetrical bending vibrations, 693-695  $\text{cm}^{-1}$  due to Si-O symmetrical bending vibrations and 777-779 and 794-796  $\text{cm}^{-1}$  due to Si-O symmetrical stretching vibrations, while the 1080-1086 and 1160-1164  $\text{cm}^{-1}$  absorption region arises from Si-O symmetrical stretching vibrations due to low Al for Si substitution. These assignments are in good agreement with the observation on the quartz mineral obtained [11]. With the view [15], the observed absorption peaks in the ranges 1610-1614 and 1870-1875  $\text{cm}^{-1}$  indicate the presence of quartz in present sediment are weathered from metamorphic origin.

### 3.3. Feldspar

Feldspar group of minerals are also frequent constituents in sediments. The feldspar groups of minerals are of several types having different compositions such as orthoclase, microcline, sanidine and albite. From this, four feldspars such as orthoclase, microcline and sanidine are having the same chemical formula ( $\text{KAlSi}_3\text{O}_8$ ). However they are differing in their structure (orthoclase-monoclinic, microcline-triclinic and sanidine-tetrahedral). The FTIR spectra are sensitive both to structural and compositional variations in the minerals. The peak pertaining in the range 585-588  $\text{cm}^{-1}$  due to O-Si-(Al)-O bending vibration in all the samples indicate the presence of microcline feldspar. The peak in the range 633-638  $\text{cm}^{-1}$  due to Al-O coordination vibration indicates the presence of orthoclase feldspar in all sites. The presence of albite in the range 1006-1010  $\text{cm}^{-1}$  ( $\text{NaAlSi}_3\text{O}_8$ ; Na- feldspar) mineral is identified in sediment ( $S_{30}$  and  $S_{53}$ ) [12].

### 3.4. Clay minerals

The presence of the bands at around 3620 and 3398-3400  $\text{cm}^{-1}$  are due to the kaolinite clay mineral [12, 16]. The intensity of the bands varies from sample to sample indicates the quantity. The observations made in the present study show that the broad absorption band at

around 3400  $\text{cm}^{-1}$  is due to OH-stretching vibration of water in the kaolinite structure. If the peaks are appeared at around 3652 and 3620  $\text{cm}^{-1}$ , the presence of kaolinite is in ordered state [12]. However, in this study, ordered state kaolinite (3652) was observed in twenty one sediment sampling sites ( $S_{13}$ - $S_{16}$ ,  $S_{20}$ ,  $S_{23}$ ,  $S_{26}$ ,  $S_{30}$ ,  $S_{36}$ ,  $S_{39}$  -  $S_{40}$ ,  $S_{43}$ ,  $S_{46}$ - $S_{48}$ ,  $S_{52}$ - $S_{53}$ ,  $S_{55}$  and  $S_{61}$ ). However only one peak is observed (3618-3621  $\text{cm}^{-1}$ ) in  $S_{13}$ - $S_{16}$ ,  $S_{20}$ - $S_{30}$ ,  $S_{36}$ ,  $S_{39}$ -  $S_{40}$ ,  $S_{43}$ ,  $S_{46}$ -  $S_{48}$ ,  $S_{52}$ - $S_{53}$ ,  $S_{55}$  and  $S_{61}$ . This indicates its disordered state.

### 3.5. Carbonate minerals

The calcite is the most common carbonate mineral in sediments. The mid infrared region (1400-1500  $\text{cm}^{-1}$ ) of the spectra is dominated by the vibrational modes of carbonate ions. When calcite mineral predominates in an aggregate, the peak is appeared in the range 1423  $\text{cm}^{-1}$  [17]. Broadening of the absorption peak in the 1423-1476  $\text{cm}^{-1}$  region to include both the aragonite and calcite band positions appears also to be related to intergrowth of the two minerals. From the existence of a diagnostic peak in 1425  $\text{cm}^{-1}$ , it is easily recognized that the calcite is present in sediment samples ( $S_7$ ,  $S_{12}$ - $S_{14}$ ,  $S_{22}$ ,  $S_{24}$ ,  $S_{29}$ ,  $S_{34}$ ,  $S_{36}$ ,  $S_{43}$ ,  $S_{52}$ - $S_{53}$ ,  $S_{58}$  and  $S_{62}$ ). Similarly, the appearance of a peak in the range 1784-1789  $\text{cm}^{-1}$  in the samples ( $S_7$ ,  $S_{12}$ - $S_{14}$ ,  $S_{22}$ ,  $S_{29}$ ,  $S_{36}$ ,  $S_{52}$ - $S_{53}$ ,  $S_{58}$  and  $S_{62}$ ) may be due to the presence of another carbonate mineral aragonite.

### 3.6. Biotite

The appearances of peak at 724  $\text{cm}^{-1}$  in the spectra of sites  $S_5$ ,  $S_9$ - $S_{11}$ ,  $S_{19}$ ,  $S_{23}$ ,  $S_{24}$ ,  $S_{26}$ ,  $S_{28}$ ,  $S_{30}$ ,  $S_{35}$ ,  $S_{41}$ ,  $S_{42}$ ,  $S_{46}$ - $S_{47}$ ,  $S_{53}$ - $S_{57}$ ,  $S_{59}$  and  $S_{60}$  are due to the presence of biotite [6, 12]. The characteristic absorption peak observed at 724  $\text{cm}^{-1}$  agrees with the peak at 724 to 728  $\text{cm}^{-1}$  observed [18].

### 3.7. Magnetic minerals

Hematite ( $\alpha$ - $\text{Fe}_2\text{O}_3$ ) is the most abundant forms of the iron containing species found in rocks and sediments [19]. The ionic replacement of Fe has been widely reported [20-22] and a variety of techniques have been employed to characterize such substituted minerals [23, 24].

In the present study the appearance of the weak absorption band in the region 570-578  $\text{cm}^{-1}$  exhibits the presence of magnetite in the sites numbers  $S_5$ ,  $S_{26}$ ,  $S_{30}$ ,  $S_{35}$ ,  $S_{42}$ ,  $S_{47}$ ,  $S_{54}$ ,  $S_{56}$ , and  $S_{57}$ . The presence of maghemite confirmed by the appearance of the peak at around 728  $\text{cm}^{-1}$  is present in the samples. The appearance of the narrow shoulder near 754  $\text{cm}^{-1}$  in the

samples of sites no. S<sub>30</sub> and S<sub>39</sub> show the presence of illite [12].

Lepidocrocite is the iron oxyhydroxide which is easily identified by the presence of OH-deformation band occur at around 546, 1022 and 1151 cm<sup>-1</sup>. There is an appearance of new peak at around 663 cm<sup>-1</sup>, which belongs to iron bearing mineral hornblende (only in sediment). Ferrihydrate is naturally occurring, poorly ordered and hydrated iron oxide mineral, which is invariably associated with silicate, and from the position of the Si-O band in the range 970-973cm<sup>-1</sup>, it is present as orthosilicate. Generally, iron oxides occur at low abundance in sediment materials than others and may be difficult, if not possible, to identify their IR spectra because of overlapping by the silicates. That is the reason for the presence of single peak. The appearance of peak at around 971cm<sup>-1</sup> from the S<sub>56</sub> indicates the presence of ferrihydrate.

### 3.8. Other minerals

The trihydratealuminium mineral gibbsite is identified by the observation of the peaks in the range 667-670 cm<sup>-1</sup> [12]. Appearing peaks at 2854 and 2924 cm<sup>-1</sup> in all the samples show the presence of organic carbon [25-28]. Chrysotile is the serpentine mineral, trioctahedral analogues of kaolinite with very different morphologies [12]. These minerals differ from kaolin minerals and are readily distinguished from each other, particularly from the OH-stretching region. This serpentine mineral is identified in S<sub>40</sub> sediment samples by their characteristic absorption bands at around 451 cm<sup>-1</sup>. The appearance of peak in the region 1394-1398 cm<sup>-1</sup> shows the presence of cerussite in sediment. Sepiolite and palygorskite are hydrous Mg silicate clay minerals with fibrous-like morphologies that typically occur as fine sediments, poorly crystalline masses. The mineral sepiolite is present in S<sub>12</sub>, S<sub>13</sub> and S<sub>62</sub> sediment samples. The presence of nacrite can be confirmed by the appearance of the peaks in the ranges 914-917 cm<sup>-1</sup> in S<sub>7</sub>, S<sub>29</sub>, S<sub>58</sub> and S<sub>62</sub> sediment samples.

The extinction co-efficient values for quartz, microcline

feldspar, orthoclase feldspar, hematite and kaolinite are calculated and the values are tabulated in Table 2. From this, it is observed that these minerals are distributed randomly. The maximum extinction co-efficient value quartz, microcline and orthoclase feldspar, hematite and kaolinite are 138.22, 67.24, 63.66, 106.72 and 157.62 in the site numbers S<sub>47</sub>, S<sub>59</sub>, S<sub>35</sub>, S<sub>56</sub> and S<sub>7</sub> respectively. The minimum extinction co-efficient value for quartz, microcline and orthoclase feldspar and hematite are 4.86, 4.04, 3.68, 2.60 and 11.82 in the site numbers S<sub>30</sub>, S<sub>31</sub>, S<sub>31</sub>, S<sub>34</sub> and S<sub>65</sub> respectively. With these upper and lower limits of the above minerals, the other sites may be arranged in an order quantitatively. In overall view, the amount of hematite and kaolinite are lesser than feldspar and very much lesser than quartz in all the sites which are visually indicated in the Fig. 3. Two moderate correlations were observed between (Ex.Q) with (Ex.MF) and (Ex. OF) with (Ex. K). It indicates sources of microcline feldspar and kaolinite may be derived from quartz and orthoclase feldspar respectively, which is shown in the Table 3.

From the XRD patterns and results, it is observed that the minerals identified in samples, quartz, orthoclase feldspar, microcline feldspar, albite feldspar, goethite, gibbsite, hematite, magnetite, kyanite, monazite, zircon, biotite, calcite, sepiolite, aragonite, hornblende, Fe-quartz and montmorillonite are observed. The reason for the absence of the few minerals in this analysis, which are identified through FT-IR, is due to the disorderedness (loss of crystalline nature) of the respective minerals. At the same time, few minerals like Fe-quartz, monazite, zircon, hornblende and kyanite are identified only in XRD analysis which indicates its crystalline order even though it is in very meager amount. However, the major minerals quartz and feldspars are present invariably in all the samples. The clay mineral kaolinite is not identified which may indicate the complete disorderedness of this mineral. The minor minerals calcite, sepiolite and aragonite and the iron bearing minerals hematite, magnetite, goethite and hornblende are identified.

**Table 2: The Extinction-coefficient of quartz, microcline feldspar, orthoclase feldspar, hematite and kaolinite for the sediment samples**

Site No.	Extinction-coefficient				
	Quartz	Microcline feldspar	Orthoclase feldspar	Hematite	Kaolinite
S <sub>1</sub>	24.12	6.51	3.68	11.97	14.30
S <sub>2</sub>	30.80	7.61	36.19	18.25	76.71
S <sub>3</sub>	41.66	8.29	44.65	19.71	82.49
S <sub>4</sub>	129.76	42.87	17.66	96.04	103.03

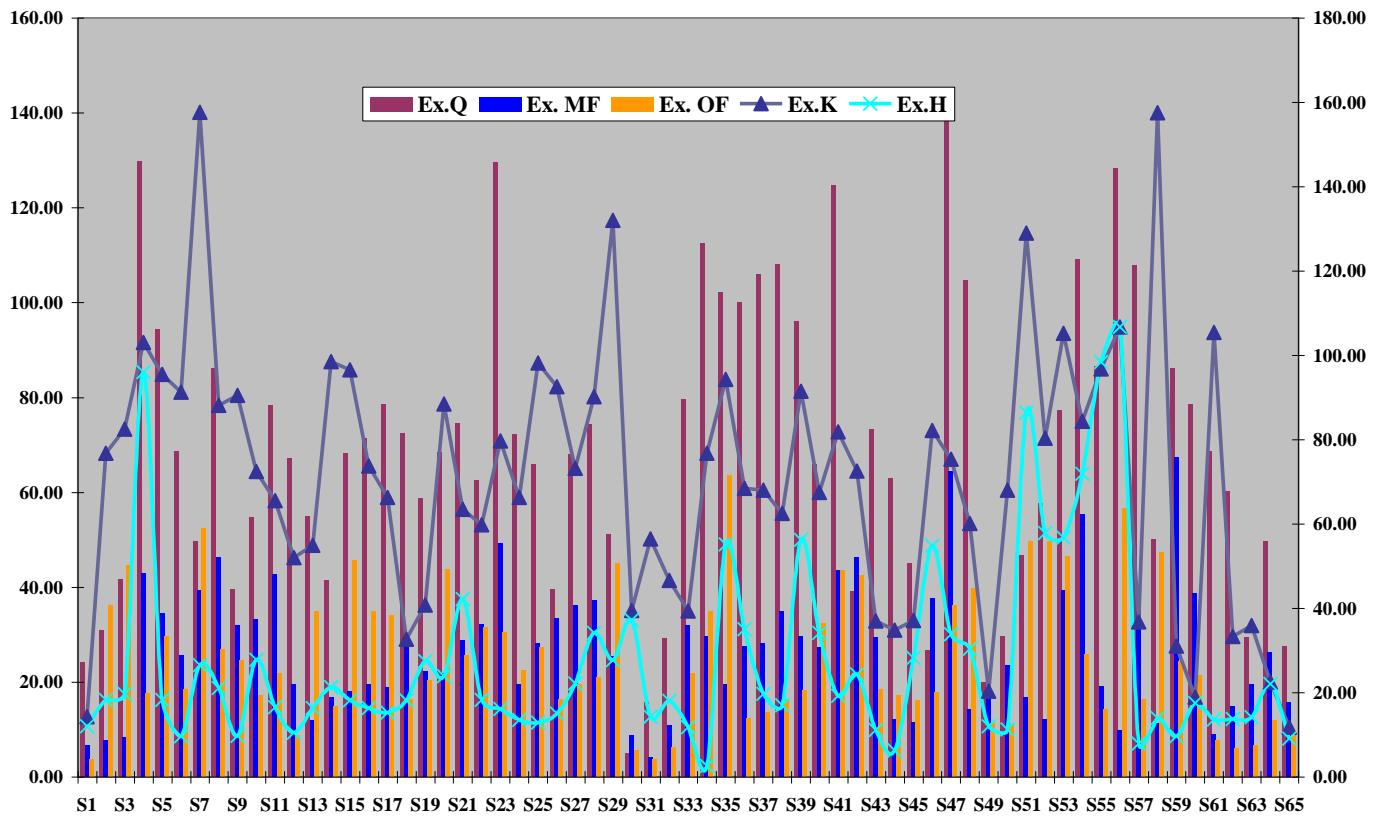
S <sub>5</sub>	94.40	34.48	29.71	18.31	95.51
S <sub>6</sub>	68.72	25.64	18.49	9.59	91.22
S <sub>7</sub>	49.70	39.18	52.33	26.49	157.62
S <sub>8</sub>	86.19	46.28	26.79	21.08	88.16
S <sub>9</sub>	39.48	31.86	24.60	9.76	90.45
S <sub>10</sub>	54.69	33.15	17.19	27.80	72.41
S <sub>11</sub>	78.28	42.69	21.67	16.59	65.49
S <sub>12</sub>	67.15	19.48	8.71	10.47	51.99
S <sub>13</sub>	54.87	11.81	34.83	16.36	54.87
S <sub>14</sub>	41.37	16.83	14.89	21.29	98.46
S <sub>15</sub>	68.11	18.02	45.73	18.14	96.49
S <sub>16</sub>	71.32	19.48	34.96	16.29	73.74
S <sub>17</sub>	78.64	18.79	33.99	15.28	66.28
S <sub>18</sub>	72.45	28.42	16.44	18.19	32.67
S <sub>19</sub>	58.69	22.32	20.38	27.49	40.74
S <sub>20</sub>	68.41	21.71	43.76	23.85	88.38
S <sub>21</sub>	74.48	28.81	25.65	42.22	63.44
S <sub>22</sub>	62.42	32.14	31.59	18.28	59.77
S <sub>23</sub>	129.61	49.28	30.42	16.07	79.71
S <sub>24</sub>	72.28	19.47	22.53	13.50	66.31
S <sub>25</sub>	65.88	28.19	27.19	12.84	98.14
S <sub>26</sub>	39.46	33.45	16.31	15.08	92.56
S <sub>27</sub>	68.01	36.18	19.46	22.14	73.18
S <sub>28</sub>	74.32	37.28	21.09	34.19	90.14
S <sub>29</sub>	50.99	25.49	44.99	27.73	131.97
S <sub>30</sub>	4.86	8.69	5.61	37.20	39.51
S <sub>31</sub>	15.80	4.04	3.68	14.24	56.46
S <sub>32</sub>	29.18	10.84	6.19	18.08	46.55
S <sub>33</sub>	79.61	31.98	21.87	11.81	39.34
S <sub>34</sub>	112.43	29.61	34.98	2.60	76.76
S <sub>35</sub>	102.18	19.44	63.66	55.09	94.30
S <sub>36</sub>	100.15	27.46	12.43	35.03	68.38
S <sub>37</sub>	105.99	28.04	13.51	19.69	68.01
S <sub>38</sub>	108.13	34.87	16.24	17.01	62.53
S <sub>39</sub>	96.14	29.56	18.19	56.20	91.49
S <sub>40</sub>	65.83	27.16	32.42	34.21	67.51
S <sub>41</sub>	124.69	43.58	43.46	19.28	81.87
S <sub>42</sub>	39.08	46.27	42.37	24.29	72.57
S <sub>43</sub>	73.18	29.49	18.43	11.12	36.96
S <sub>44</sub>	62.98	12.16	17.20	6.30	34.78
S <sub>45</sub>	45.07	11.45	16.04	28.19	37.13
S <sub>46</sub>	26.67	37.56	17.82	54.80	82.12
S <sub>47</sub>	138.22	64.39	36.25	33.84	75.30
S <sub>48</sub>	104.77	14.34	39.73	30.35	60.13
S <sub>49</sub>	19.85	17.18	11.27	11.97	20.38
S <sub>50</sub>	29.61	23.55	11.12	11.19	68.00
S <sub>51</sub>	46.74	16.74	49.55	86.42	128.97
S <sub>52</sub>	57.65	12.22	49.73	57.81	80.30
S <sub>53</sub>	77.31	39.18	46.51	56.72	105.18
S <sub>54</sub>	109.04	55.27	25.83	71.87	84.29
S <sub>55</sub>	86.49	19.07	14.33	98.41	96.74
S <sub>56</sub>	128.30	9.92	56.54	106.72	106.74
S <sub>57</sub>	107.82	38.42	16.28	7.84	36.70

S <sub>58</sub>	50.16	11.34	47.25	13.95	157.47
S <sub>59</sub>	86.12	67.24	24.38	9.61	31.01
S <sub>60</sub>	78.50	38.69	21.30	17.48	18.91
S <sub>61</sub>	68.69	9.08	7.69	13.62	105.43
S <sub>62</sub>	60.29	14.78	5.99	13.68	33.32
S <sub>63</sub>	29.48	19.42	6.49	14.18	35.88
S <sub>64</sub>	49.67	26.33	11.81	22.07	22.49
S <sub>65</sub>	27.54	15.74	9.12	9.04	11.82
<b>Average</b>	<b>68.68</b>	<b>26.63</b>	<b>25.56</b>	<b>27.34</b>	<b>71.25</b>
<b>Maximum</b>	<b>138.22</b>	<b>67.24</b>	<b>63.66</b>	<b>106.72</b>	<b>157.62</b>
<b>Minimum</b>	<b>4.86</b>	<b>4.04</b>	<b>3.68</b>	<b>2.60</b>	<b>11.82</b>

**Table 3: Pearson correlation coefficient matrix among the parameters for sediment samples**

	Ex. Q	Ex. MF	Ex. OF	Ex. K	Ex. H
Ex. Q	1.00				
Ex. MF	0.52	1.00			
Ex. OF	0.30	0.10	1.00		
Ex. K	0.19	0.09	0.60	1.00	
Ex. H	0.29	0.04	0.31	0.40	1.00

Ex. Q, Ex. MF, Ex. OF, Ex. K and Ex. H are the extinction co-efficient of quartz, microcline feldspar, orthoclase feldspar, Kaolinite, and hematite respectively



(Ex. Q, Ex. MF, Ex. OF, Ex. K and Ex. H respectively represent extinction coefficient of quartz, microcline feldspar, orthoclase feldspar, kaolinite and hematite)

**Fig. 3: Extinction coefficient of major minerals (quartz, microcline and orthoclase feldspar, kaolinite and hematite) of all sites.**

#### 4. CONCLUSION

Mineralogical characterization the samples were analyzed through FTIR and XRD methods. Twenty three mineral such as quartz, feldspar in different composition (orthoclase, microcline and albite), hematite, Kaolinite, palygroskite, magnetite, maghemite, biotite, gibbsite, montmorillonite, calcite, aragonite, illite, lepidocrocite, ferrihydrate, hornblende, nacrite, sepiolite, chrysotile, cerussite and organic carbon were observed are observed through FTIR. Among all these minerals, quartz is invariably present in all the study samples. The origin of quartz is determined using the characteristic peaks  $1610-1614\text{ cm}^{-1}$ . The obtained results show the presence of quartz in the Kalrayan hills and are from metamorphic origin. From the calculated extinction coefficient values, the amount of hematite and kaolinite are lesser than feldspar and very much lesser than quartz in all the sites. From XRD analysis, the minerals such as monazite and zircon are additionally identified. Some of the minerals observed through FTIR analysis are not identified in XRD study which indicates its loss of crystalline nature.

#### 5. REFERENCES

1. Ant3no Mateus, Jorge Figueiras, Ivo Martins, Pedro C. Rodrigues and Filipe Pinto, *Minerals*, 2020; **10**:551.
2. Ramasamy V, Senthil, S. *Bulletin of Pure and Applied Sciences*, 2009; **28(1)**:1-6.
3. Schmidt C. *Geochim. Cosmochim. Acta* 2018; **220**:499-511.
4. Schmidt C, Romer R.L, Wohlgemuth-Ueberwasser C.C, Appelt O. *Ore Geol. Rev.* 2020; **117**:103263.
5. Ramasamy V, Suresh G, Rajkumar P, Murugesan S, Mullainathan S, Meenakshisundaram V. *J. Radioanal. Nucl. Chem.*, 2011; **292**:381-393.
6. John M, Hunt, Mary P, Wishard, Lawrence C, Bonham. *Analytical Chemistry*, 1950; **22(12)**:1478.
7. Tuddenham WM, Lyaon RJP. *Analytical Chemistry*, 1960; **32**:1630-1634.
8. Stubican V, Roy RZ. *Kristallogr. Kristallogeom*, 1961a; **115**:200-214.
9. Farmer VC, Russell J.D. *Spectro Chemical Acta*, 1964; **20**:1149-1173.
10. Russell JD, Farmer V.C, Velde B. *Mineralogical Magazine*, 1970; **37**:869-879.
11. Hlavay J, Jonas K, Elet, Inczedy S, J. *Clays and Clay Minerals*, 1978; **26(2)**:139.
12. Russell JD, Ed. by Wilson M.J, *Blackie and Son Ltd.*, New York, 1987; 133.
13. Madejova J. *Vibrational Spectroscopy*, 2003; **31**:1.
14. Ramasamy V, Paramasivam K, Suresh G, Jose M.T. *Journal of Environmental Radioactivity*, 2014; **127**:64-74.
15. Keller WD, Pickett EE. *The American Mineralogist*, 1949; **34**:855-868.
16. Ramaswamy K, Venkatachalapathy R. *Indian Journal of Pure and Applied Physics*, 1992; **30**:171.
17. Adler HH, Kerr PF. *American Mineralogist*, 1962; **47**:700.
18. Ghosh SN. *Journal of Material Science*, 1978; **13**:1877-1886.
19. Fysh SA, Fredericks PM. *Clays and Clay Minerals*, 1983; **31(5)**:377-381.
20. Norrish K, Taylor RM. *Journal of Soil Science*, 1961; **12**:294-306.
21. Schwertmann U, Taylor RM. *Soil science society of America, Inc., Madison*, 1977; 145.
22. Yariv SH, Mendelovici E. *Applied Spectroscopy*, 1979; **33(4)**:410-411.
23. Fysh SA, Clark PE. *Physics and Chemistry of Minerals*, 1982a; **8**:180-187.
24. Fysh SA, Clark PE. *Physics and Chemistry of Minerals*, 1982b; **8**:257-267.
25. Bain D.C, Fraser A.R. *Clay Minerals*, 1984; **26**:69-76.
26. Dios CG, Romero TE, Huertas FJ, Hernandez LA, Sanchez RF. *Clays and Clay minerals*, 1996; **44(2)**:70-80.
27. Song Z, Chouparova E, Jones KW, Feng H, Marinkovic N.S. *Science Highlights*, 2001; 112-116.
28. Mohammed H, Salah K, Abdellah A, Abdelaziz El B, Mohamed Wl M. *Applied Clay Science*, 2001; **20**:1-12.